Cancer Cell, Volume *31*

Supplemental Information

Chemosensitive Relapse in Small Cell Lung Cancer Proceeds through an EZH2-SLFN11 Axis

Eric E. Gardner, Benjamin H. Lok, Valentina E. Schneeberger, Patrice Desmeules, Linde A. Miles, Paige K. Arnold, Andy Ni, Inna Khodos, Elisa de Stanchina, Thuyen Nguyen, Julien Sage, John E. Campbell, Scott Ribich, Natasha Rekhtman, Afshin Dowlati, Pierre P. Massion, Charles M. Rudin, and John T. Poirier

Supplemental Data

Table S1 (related to Figure 1). PDX line characteristics used throughout study.

Text ID	Source	Patient Diagnosis	PDX Diagnosis	Treatment	Site	Reference
JHU-LX22	Johns Hopkins University	SCLC	SCLC	none	pleura	(Hann et al., 2008)
JHU-LX33	Johns Hopkins University	SCLC	SCLC	none	transbronchial	(Hann et al., 2008)
JHU-LX44	Johns Hopkins University	SCLC	SCLC	unknown	unknown	(Poirier et al., 2013)
JHU-LX48	Johns Hopkins University	SCLC	SCLC	platinum	unknown	(Poirier et al., 2013)
JHU-LX101	Johns Hopkins University	SCLC	SCLC	none	transbronchial	(Leong et al., 2014)
JHU-LX102	Johns Hopkins University	SCLC	SCLC	none	transbronchial	(Leong et al., 2014)
JHU-LX108	Johns Hopkins University	SCLC	SCLC	carboplatin, radiation	transbronchial	(Leong et al., 2014)
JHU-LX110	Johns Hopkins University	SCLC	SCLC	none	transbronchial	(Leong et al., 2014)
SCRX-Lu149	StemcentRx, Inc.	SCLC	SCLC	none	lung	(Saunders et al., 2015)
MSK-LX40	Memorial Sloan Kettering Cancer Center	SCLC	SCLC	C/E	lung	new
MSK-LX95	Memorial Sloan Kettering Cancer Center	SCLC	SCLC	C/E	lung	new

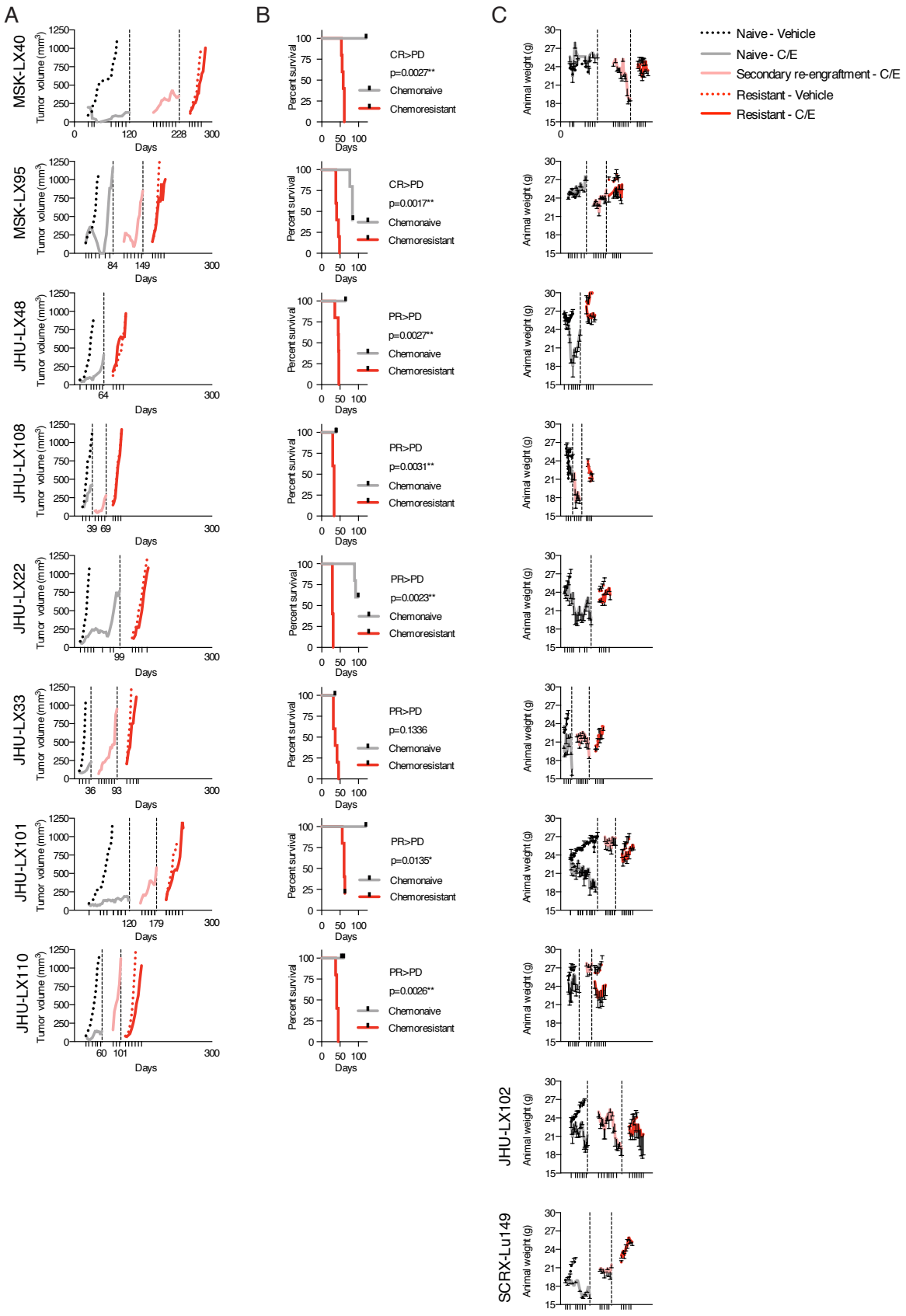
A
B
C
MSK-LX40
MSK-LX95
JHU-LX48
JHU-LX108
JHU-LX22
JHU-LX33
JHU-LX101
JHU-LX110
JHU-LX102
SCRX-Lu149
Tumor volume (mm³)
Days
Percent survival
Animal weight (g)
CR>PD
p=0.0027**
CR>PD
p=0.0017**
PR>PD
p=0.0027**
PR>PD
p=0.0031**
PR>PD
p=0.0023**
PR>PD
p=0.1336
PR>PD
p=0.0135*
PR>PD
p=0.0026**
Chemonaive
Chemoresistant
Naive - Vehicle
Naive - C/E
Secondary re-engraftment - C/E
Resistant - Vehicle
Resistant - C/E

Figure S1 (related to Figure 1). Modeling acquired resistance to C/E in PDX models of SCLC.
(A) Average tumor volume curves for 10 models included in study. n=5/arm, per PDX. Data per treatment group reported as means for clarity. Dashed lines indicate points on study where cisplatin/etoposide (C/E) treated cohorts were collected and re-engrafted (pooled fashion) into additional cohorts of animals. JHU-LX102 and SCRX-Lu149 data were included in Figure 1C, thus are omitted in these panels. Color legend for entire figure on far right.
(B) Survival for chemonaive and chemoresistant versions of models on C/E treatment. Model chemosensitivity conversion status (>) indicated above p values from log-rank (Mantle-Cox) tests; CR=complete response, PR=partial response, PD=progressive disease. Survival is shown as time on study to reach the pre-specified volumetric endpoint of 1,000 mm^3. Survival data points were censored if volumetric endpoints were not reached on protocol (~1,000 mm^3), serious weight loss was encountered (>20% body weight at point of randomization), or total cycles of C/E reached tolerability endpoint (~8 weekly cycles).
(C) Animal weights on study. Data are reported as mean ± SEM; n=5/arm.

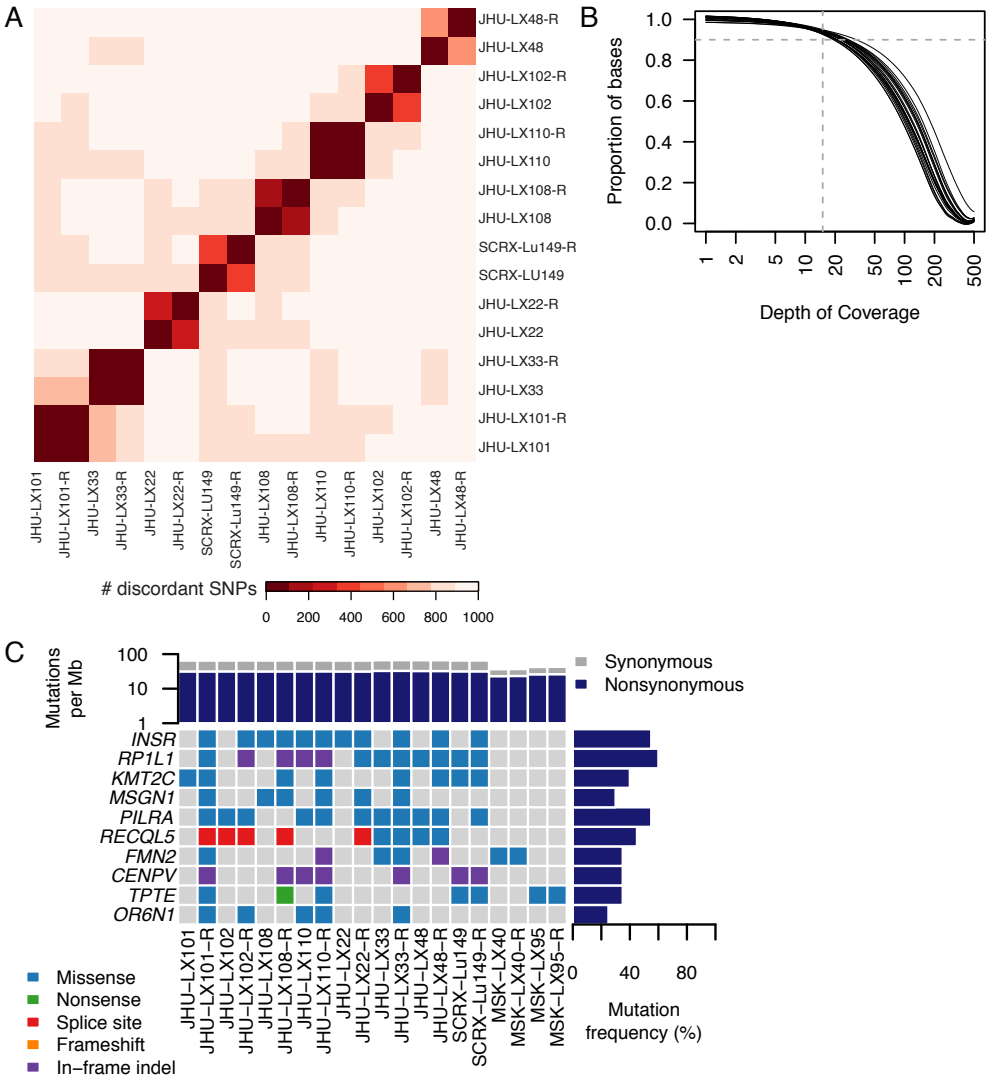

Figure S2 (related to Figure 2). Whole exome sequencing of paired naive and resistant PDX pairs.
(A) Concordance of genotypes for >1,000 common single nucleotide polymorphisms (SNPs) across naive and resistant pairs. Color scale below.
(B) Proportion of bases in the exome capture region covered to a given read depth. The intersection of the horizontal (90%) and the vertical lines (15) indicate the minimum depth used to call mutations using MuTect2.
(C) A mutation plot indicating the most common mutations occurring in the chemoresistant setting ordered by frequency. Mutation legend shown below.

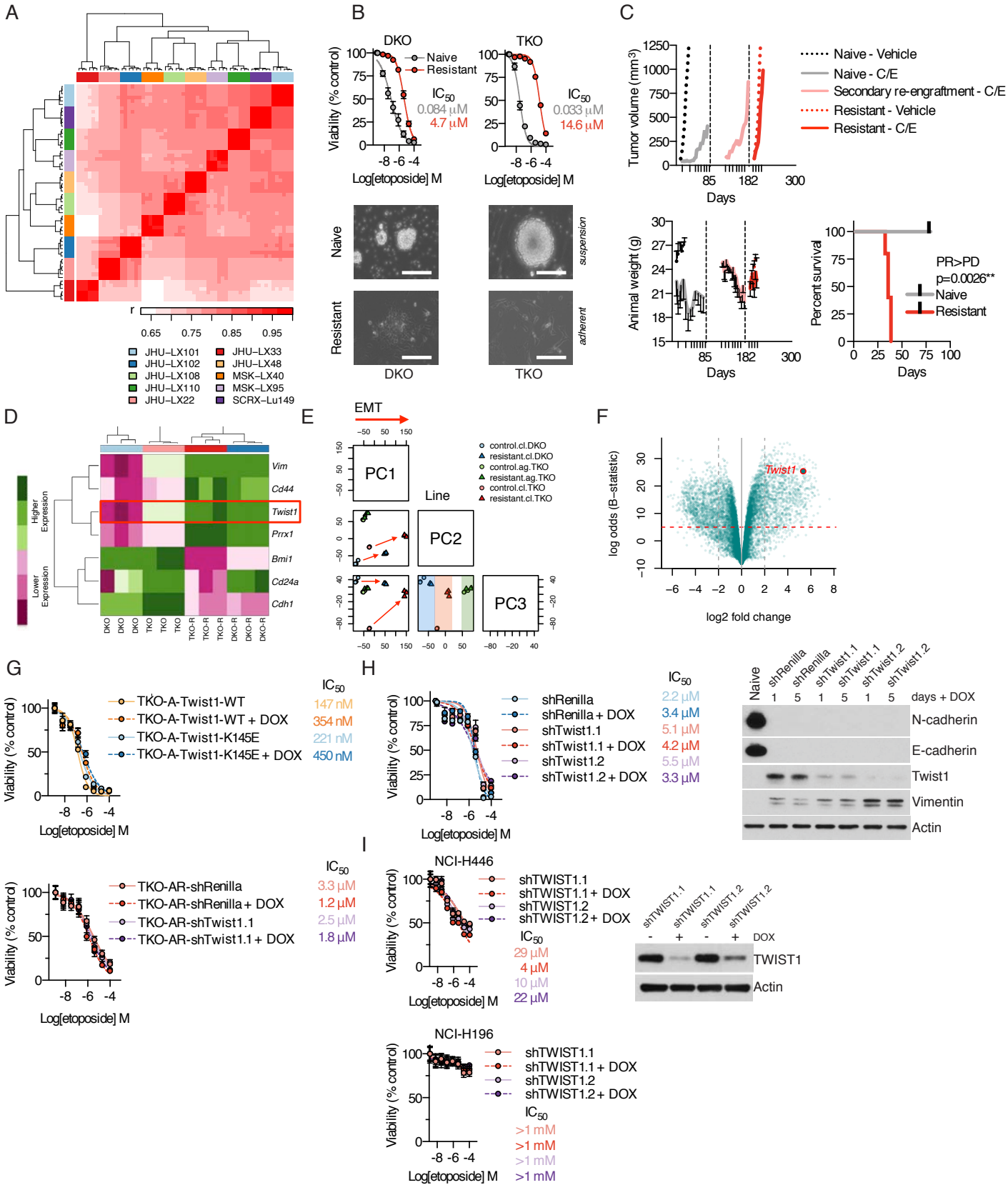
A
r
0.65 0.75 0.85 0.95
JHU–LX101
JHU–LX102
JHU–LX108
JHU–LX110
JHU–LX22
JHU–LX33
JHU–LX48
MSK–LX40
MSK–LX95
SCRX–Lu149
B
DKO
TKO
Naive
Resistant
Viability (% control)
IC50
0.084 μM
4.7 μM
0.033 μM
14.6 μM
Log[etoposide] M
suspension
adherent
C
Tumor volume (mm3)
Days
Naive - Vehicle
Naive - C/E
Secondary re-engraftment - C/E
Resistant - Vehicle
Resistant - C/E
Animal weight (g)
Percent survival
PR>PD
p=0.0026**
D
Vim
Cd44
Twist1
Prrx1
Bmi1
Cd24a
Cdh1
Higher Expression
Lower Expression
E
EMT
PC1
PC2
PC3
Line
control.cl.DKO
resistant.cl.DKO
control.ag.TKO
resistant.ag.TKO
control.cl.TKO
resistant.cl.TKO
F
Twist1
log odds (B–statistic)
log2 fold change
G
TKO-A-Twist1-WT
TKO-A-Twist1-WT + DOX
TKO-A-Twist1-K145E
TKO-A-Twist1-K145E + DOX
147 nM
354 nM
221 nM
450 nM
TKO-AR-shRenilla
TKO-AR-shRenilla + DOX
TKO-AR-shTwist1.1
TKO-AR-shTwist1.1 + DOX
3.3 μM
1.2 μM
2.5 μM
1.8 μM
H
shRenilla
shRenilla + DOX
shTwist1.1
shTwist1.1 + DOX
shTwist1.2
shTwist1.2 + DOX
2.2 μM
3.4 μM
5.1 μM
4.2 μM
5.5 μM
3.3 μM
Naive
shRenilla
shTwist1.1
shTwist1.2
days + DOX
N-cadherin
E-cadherin
Twist1
Vimentin
Actin
I
NCI-H446
shTWIST1.1
shTWIST1.1 + DOX
shTWIST1.2
shTWIST1.2 + DOX
29 μM
4 μM
10 μM
22 μM
DOX
TWIST1
Actin
NCI-H196
>1 mM
>1 mM
>1 mM
>1 mM

Figure S3 (related to Figure 3). TWIST1 is upregulated in multiple models of chemoresistant SCLC.
(A) Hierarchical clustering of correlation coefficients, r, from RNA-seq data on biological triplicates of chemonaive and chemoresistant paired PDX samples. n=3 replicates per model per setting; n=60 data columns/rows. Color legend and scale below.
(B) Shift in etoposide sensitivity from in vitro acquired resistance modeling in DKO and TKO mSCLC cell lines. Change in morphologic appearance and culture conditions of chemonaive (suspension/spheroid) and chemoresistant (adherent) cell lines. Scale bars set to 200 μm. Experimental results are shown for 72 hr post-dose of etoposide; n=3/data point; mean viability ± SEM.
(C) Average tumor volume plot for triple knock-out allograft (TKO-A) mSCLC model; treatment arms indicated in legend on right. Points of re-transplant are indicated along the x-axis with vertical dashed lines. Day 1 of C/E cycles are indicated as vertical ticks along the x-axis. The same schedule and treatment criteria of C/E used to generate chemoresistant PDXs was used to generate chemoresistant TKO-A (TKO-AR). Below: Average animal weights on study ± SEM; n=5/arm. Below right: survival of naive versus resistant C/E-treated cohorts of mSCLC TKO allograft (TKO-A) models. Model conversion from partial response (PR) to progressive disease (PD) indicated in margin. P value from log-rank (Mantle-Cox) test.
(D) Relative expression for select genes involved in EMT between naive or parental (P) and resistant (R) cell lines, calling out *Twist1* (red box). Gene expression intensity legend on far left.
(E) Principal component (PC) analysis for naive and resistant versions of mSCLC models broken down by component. The first component of epithelial-mesenchymal transition (EMT) is shown. Legend colors and shapes shown for cell lines (cl) and allograft (ag).
(F) Volcano plot for differential gene expression across all mSCLC paired naive/parental as compared to resistant models (pooled analysis). Significance of differential expression (dashed vertical line; log2 fold change >2) and log odds beta (B) statistic (red dashed horizontal line; 5) indicated on plot. *Twist1* data point highlighted in red.
(G) Conditional gain of *Twist1* or the K145E DNA-binding mutant of *Twist1* in the naive setting or conditional suppression of *Twist1* in the resistant setting of the TKO allograft (TKO-A/AR) and influence on chemosensitivity. Conditional expression was initiated when doxycycline (DOX) was added to the culture media at 1 μg/mL, every other day, for 5 days before re-plating for viability experiments. Experimental results are shown for 72 hr post-dose of etoposide. n=3/data point, mean ± SEM.
(H) Conditional suppression of *Twist1* in the resistant DKO cell line (DKO-R) and influence on chemosensitivity. Experimental results shown for 72 hr post-dose of etoposide. n=3/data point, mean ± SEM. On right, conditional suppression of *Twist1* and effects on EMT-associated changes in protein expression of E-cadherin, N-cadherin and vimentin. Western blots for resistant DKO (DKO-R) cells on doxycycline (1 μg/mL) for 1 or 5 days before collection of samples for Western blot.
(I) Conditional suppression of *TWIST1* in the TWIST1^{HIGH} human SCLC cell lines NCI-H446 and NCI-H196 and influence on sensitivity to etoposide. Doxycycline (DOX) was added to the culture media at 1 μg/mL every other day for 5 days before re-plating for viability experiments. Experimental results are shown for 72 hr post-dose of etoposide. Two independent *TWIST1* shRNAs were tested for target suppression at 72 hr after a single dose (1 μg/mL) of doxycycline (DOX) in NCI-H446, using shTWIST1.1 for both conditional cell line experiments. n=3/data point, mean ± SEM.

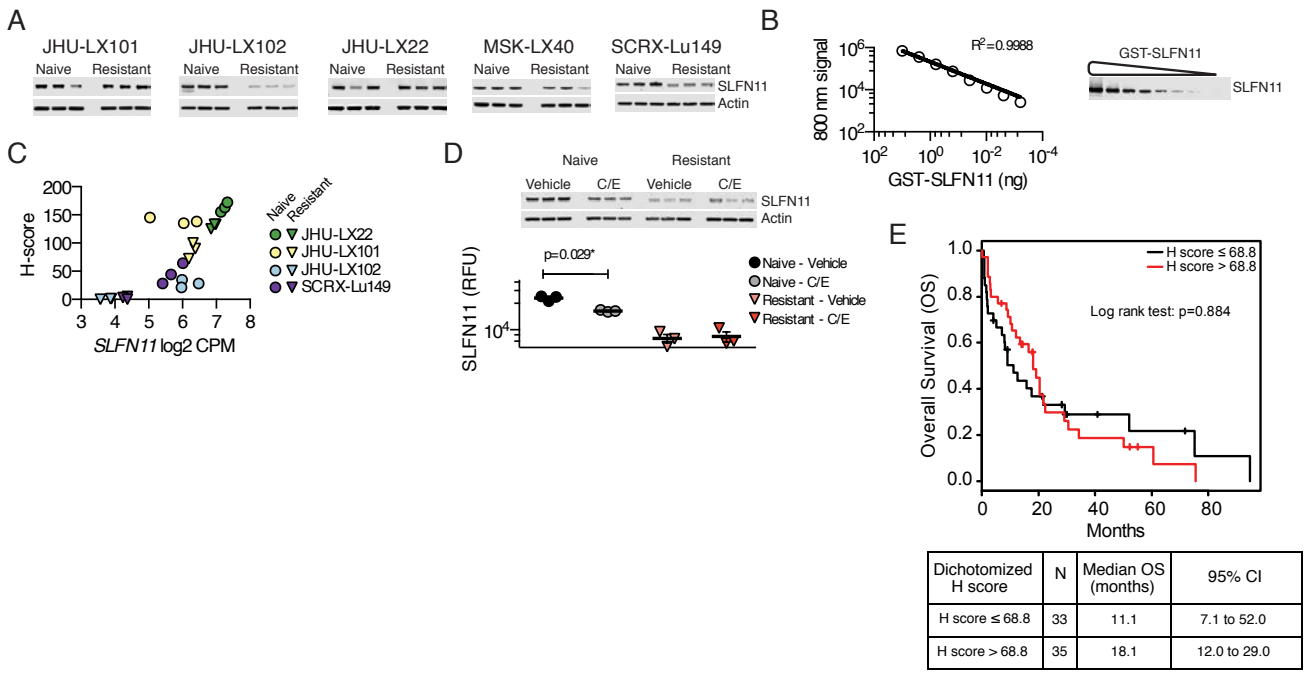

Dichotomized H score	N	Median OS (months)	95% CI
H score ≤ 68.8	33	11.1	7.1 to 52.0
H score > 68.8	35	18.1	12.0 to 29.0

Figure S4 (related to Figure 4). SLFN11 is downregulated in multiple models of chemoresistant SCLC.
(A) Western blot images from triplicate chemonaive and resistant PDX tumor samples used for calculating data included in Figure 4G, normalizing SLFN11 signal (800 nm) to actin (700 nm). Three tumor replicates analyzed per setting.
(B) Standard curve for detection of recombinant SLFN11 establishes conservative upper and lower limits of detection in pure versus crude experimental samples; recombinant GST-tagged SLFN11 (GST-SLFN11). Standard curve R^2 value of 0.9988.
(C) RNA-seq versus SLFN11 H-score for available PDX naive and resistant tumors. Paired triplicates are color-coded in the naive (circles) or resistant (downward triangle) and correspond to the color grid use in Figure 3A.
(D) Change in tumor SLFN11 expression from vehicle or C/E-treated arms of chemonaive or chemoresistant SCRX-Lu149 model. SLFN11 relative fluorescence units (RFU) as a function on time on treatment in PDX model SCRX-Lu149. P value shown for paired t-test. Mean ± SD.
(E) Survival of SCLC by dichotomized H-score. The best cutoff of H-score for predicting objective response rate (ORR) is 68.8 based on maximizing the Youden's J index (J =sensitivity + specificity – 1). Inset table below shows usable clinical cases from H-score on TMAs analyzed in aggregate.

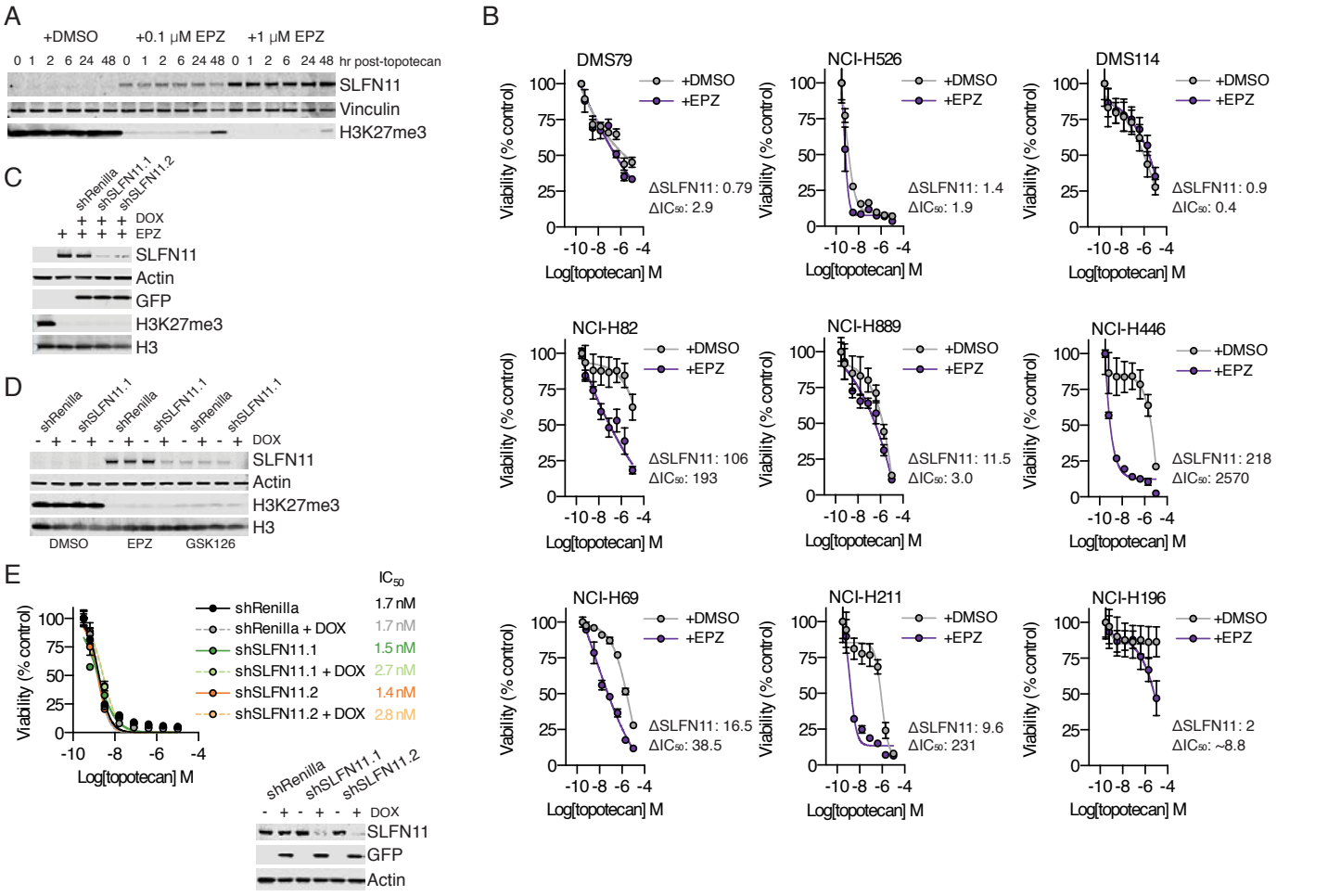

Figure S5 (related to Figure 5). SLFN11 is re-expressed in SCLC following chemical EZH2 inhibition.

(A) NCI-H82 cell line was treated for 7 days with DMSO, 100 nM or 1 μM EPZ in culture, adding EPZ every day. Cells were then exposed to 1 μM topotecan for 1 hr, washed and then released into fresh media for a 48 hr collection period. Indicated time points in hours shown above for Western blot.

(B) Individual IC_{50} curve traces for the 9 human SCLC cell lines used for plotting data in Figure 5G. Cells were split every 3 days, adding 1 μM EPZ or vehicle (DMSO) every day for 7 days, before plating 1-5x10^4 cells for determining 72 hr viability. Changes in SLFN11 protein expression and best fits of topotecan IC_{50} values shown per cell line. n=3/data point, mean ± SEM. Experiments were repeated three times, with a representative set of replicates shown.

(C) NCI-H82 treated with 1 μM EPZ in culture for 7 days with or without a 72 hr co-treatment period with 1 μg/mL doxycycline (DOX). Two independent shRNAs targeting SLFN11 are shown (shSLFN11.1 and shSLFN11.2) versus a non-targeting shRenilla control.

(D) SLFN11 re-expression under different EZH2 chemical inhibitors. NCI-H82 treated in culture for 7 days with DMSO, 1 μM EPZ or 1 μM GSK126 with or without a 72 hr co-treatment period with 1 μg/mL doxycycline (DOX) to induce shRNA against *SLFN11* or Renilla luciferase before analyzing by Western blot.

(E) Conditional shRNA suppression of *SLFN11* in the SLFN11^{HIGH} SCLC cell line NCI-H526 and effect on chemosensitivity. As in Figure 5H, 1 μg/mL doxycycline (DOX) was added to cell lines for 3 days before re-plating for viability assays. IC_{50} values colored according to arm. Two independent shRNAs against *SLFN11* were tested prior to experiments (shSLFN11.1 and shSLFN11.2) as well as an shRNA targeting Renilla luciferase (shRenilla) shown in Western blot. GFP is co-expressed from an independent promoter upon exposure to doxycycline in pLT3GEPIR, which was the common backbone for all shRNA experiments (Fellmann et al., 2013). n=3/data point, mean ± SEM.

Table S2 (related to Figure 6). Summary of described resistance mechanisms observed in PDX models and efficacy of chemical EZH2 inhibition.

PDX	Chemonaive C/E response	Chemoresistant C/E Response	*TWIST1*	*SLFN11*	EPZ efficacy
JHU-LX22	PR	PD	-	decrease	NR
JHU-LX33	PR	NR	increase	-	-
JHU-LX44	NR	NR	-	-	PR
JHU-LX48	PR	PD	-	-	PR
JHU-LX101	PR	PD	-	-	-
JHU-LX102	PD	PD	-	decrease	PR
JHU-LX108	PR	PD	increase	-	NR
JHU-LX110	PR	PR	-	-	-
MSK-LX40	CR	PD	-	decrease	-
MSK-LX95	CR	PD	increase	-	-
SCRX-Lu149	PR	PD	-	decrease	PR

CR=complete response, PR=partial response, PD=progressive disease, NR=no response

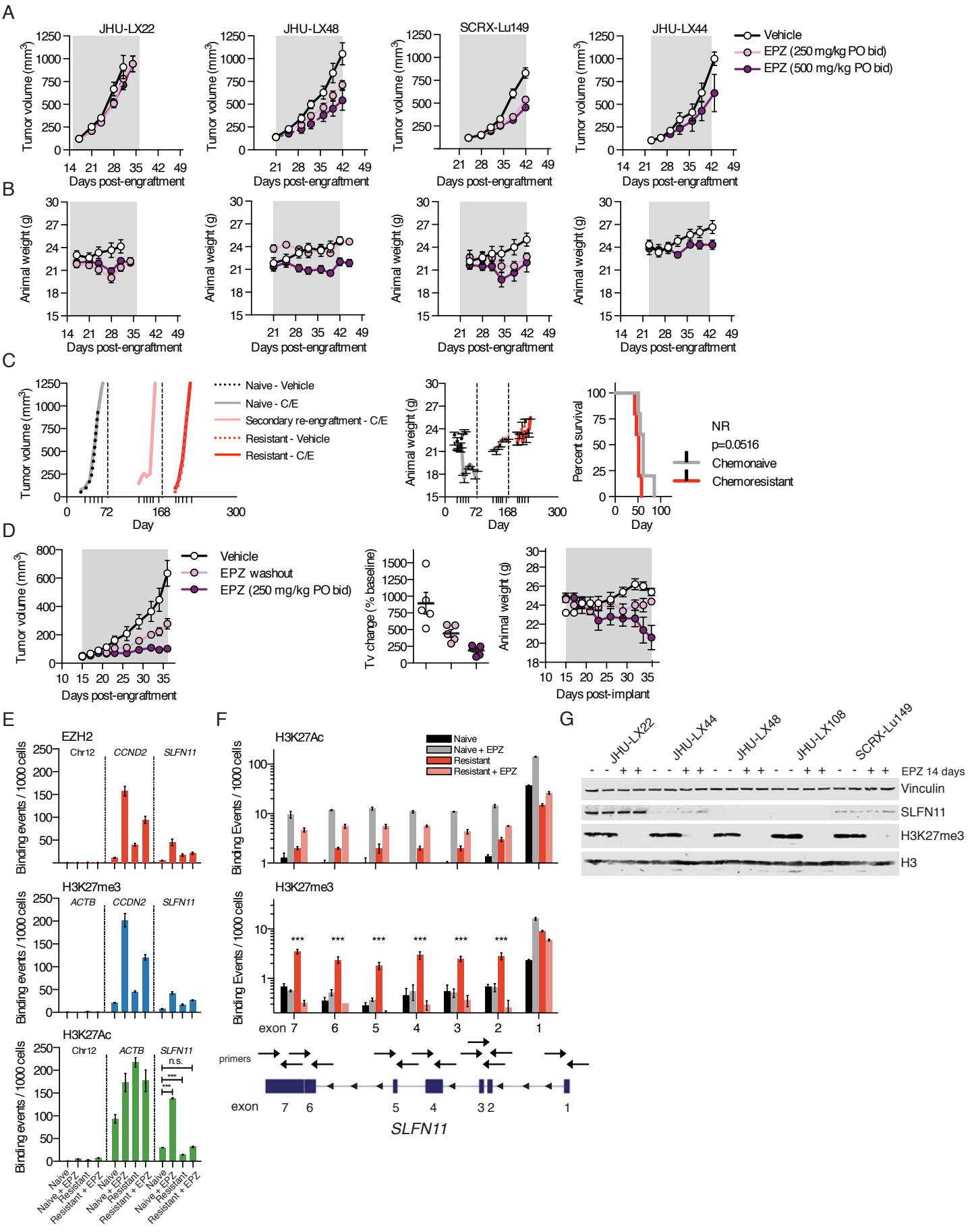
A
JHU-LX22
JHU-LX48
SCRX-Lu149
JHU-LX44
Tumor volume (mm3)
Days post-engraftment
Vehicle
EPZ (250 mg/kg PO bid)
EPZ (500 mg/kg PO bid)
B
Animal weight (g)
Days post-engraftment
C
Tumor volume (mm3)
Day
Naive - Vehicle
Naive - C/E
Secondary re-engraftment - C/E
Resistant - Vehicle
Resistant - C/E
Animal weight (g)
Percent survival
NR
p=0.0516
Chemonaive
Chemoresistant
D
Tumor volume (mm3)
Days post-engraftment
Vehicle
EPZ washout
EPZ (250 mg/kg PO bid)
Tv change (% baseline)
Animal weight (g)
Days post-implant
E
EZH2
Chr12
CCND2
SLFN11
Binding events / 1000 cells
H3K27me3
ACTB
CCDN2
H3K27Ac
n.s.
Naive
Naive + EPZ
Resistant
Resistant + EPZ
F
H3K27Ac
Binding Events / 1000 cells
H3K27me3
exon 7 6 5 4 3 2 1
primers
exon 7 6 5 4 3 2 1
SLFN11
G
JHU-LX22
JHU-LX44
JHU-LX48
JHU-LX108
SCRX-Lu149
EPZ 14 days
Vinculin
SLFN11
H3K27me3
H3

Figure S6 (related to Figure 6). EZH2 chemical inhibition restores SLFN11 expression after silencing during acquired resistance.

(A) Single agent activity of EPZ across four PDX models, using two separate dose schedules. Areas in grey represent time on continuous oral, twice a day (PO bid) treatment. EPZ was administered on a 10 AM/6 PM schedule, 7 days a week for 14-21 days, depending on tumor growth kinetics during treatment. Tumor volumes reported as mean ± SEM; n=7-8 per arm. The 250 mg/kg PO bid arm for JHU-LX44 was not performed. All tumors used for these experiments were of chemonaive origin, where applicable.

(B) Average weight ± SEM for animals in (A).

(C) C/E efficacy in chemorefractory model JHU-LX44. Mean tumor volume ± SEM (n=5/arm), animal weights, and survival as a function of time to reach a volumetric endpoint of 1,000 mm^3 as in Figure 1 and S1. Color legend on right.

(D) Repeated exposure to EPZ in vivo in SCRX-Lu149. Left: efficacy of continuous dosing through a re-engraftment period. Tumors at the end of a three-week efficacy experiment for SCRX-Lu149 (from Figure S6A) were engrafted from either vehicle or 250 mg/kg PO bid treatment arms into mice. Two weeks following engraftment, mice from previously treated tumors were treated with vehicle (washout) or EPZ for an 3 additional weeks; Data reported as average tumor volume ± SEM; n=5/arm. Color legend used for panel on right. Middle: Comparison of tumor volume change (Tv change) at week 3 on treatment versus volumes at treatment initiation (baseline) per group. Individual Tv change points shown with mean ± SEM per indicated arm. Right: Average animal weight on study for left panel. Continuous treatment arm approached limits of protocol weight loss (~20% body weight from randomization).

(E) ChIP-qPCR for *SLFN11* (upstream of first exon) in various tumor samples use in Figure 6 as compared to positive and negative control primer pairs. ChIP target indicated in color: EZH2 (red), H3K27me3 (blue) and H3K27Ac (green). Each ChIP-qPCR series is shown for three targets in the order of negative control, positive control and *SLFN11* (left-to-right): Chr12 refers to a gene desert region in chromosome 12, not known to bind any transcription factor (Active Motif; 71001). P value indices (***<0.0001) reported for paired t-tests between groups within the H3K27Ac (green) sample set; n.s.=non-significant; n=3 replicates per condition, mean ± SD.

(F) ChIP-qPCR for *SLFN11* in an exon-by-exon fashion in various tumor samples use in Figure 6. ChIP targets H3K27Ac (above) and H3K27me3 (below). Indicated exons along bottom x-axis. n=3 replicates per condition, mean ± SD. P value indices (***<0.0001) reported for paired t-tests between resistant SCRX-Lu149 samples and all other sample test sets; n.s.=non-significant. Exon model for *SLFN11* locus shown below with indicated primer pairs used to interrogate specific exons. Exon model used for illustrative purposes and not to any scale.

(G) Western blot analysis from 5 chemonaive PDX models treated with vehicle (-) or 250 mg/kg EPZ PO bid (+) for 14 days before collection of tissues. Two tumors examined per arm, per PDX at day 14 on study.

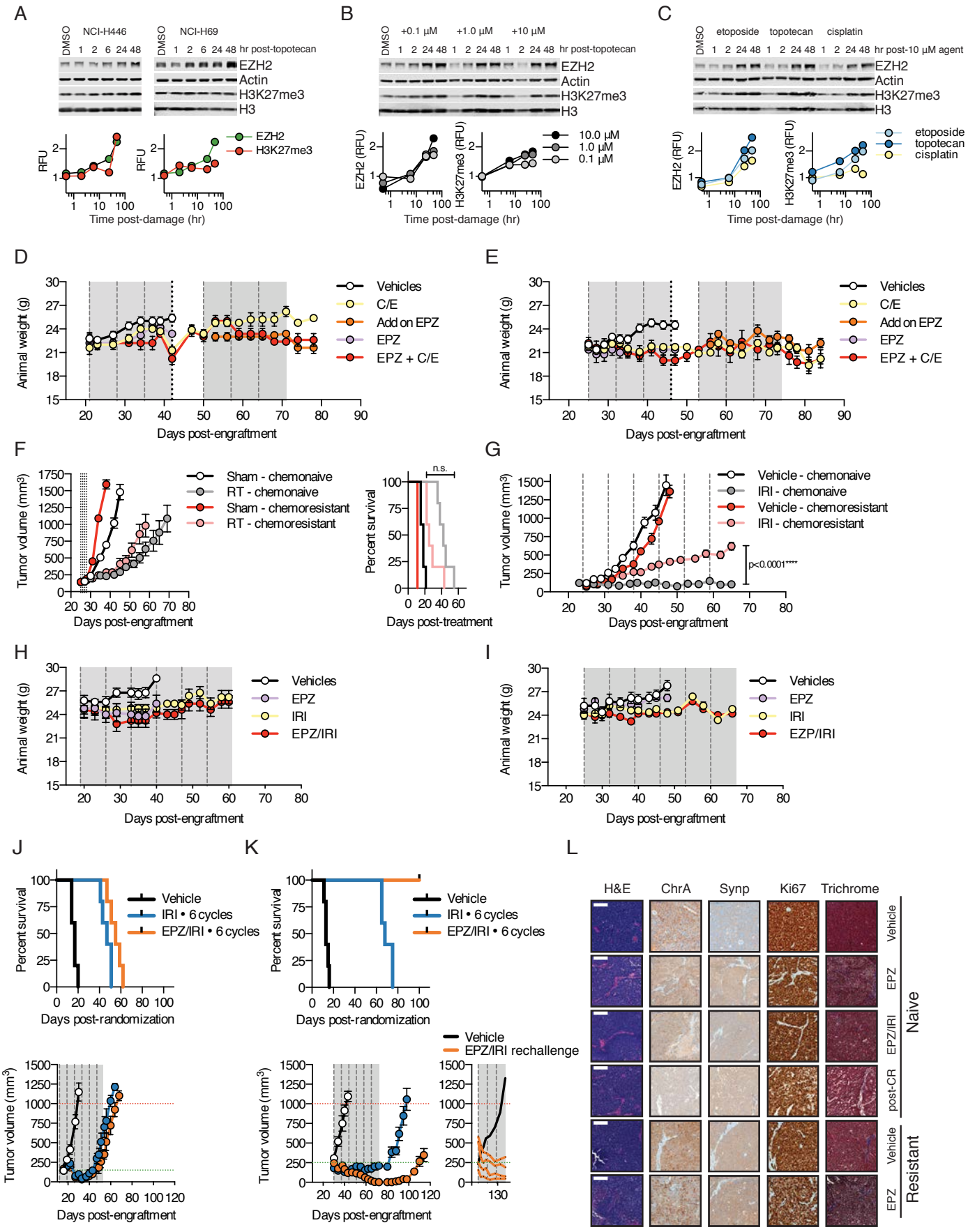
A
DMSO
NCI-H446
NCI-H69
1 2 6 24 48 hr post-topotecan
EZH2
Actin
H3K27me3
H3
RFU
Time post-damage (hr)
B
DMSO
+0.1 μM
+1.0 μM
+10 μM
1 2 24 48 hr post-topotecan
EZH2 (RFU)
H3K27me3 (RFU)
10.0 μM
1.0 μM
0.1 μM
C
DMSO
etoposide
topotecan
cisplatin
1 2 24 48 hr post-10 μM agent
etoposide
topotecan
cisplatin
D
Animal weight (g)
Days post-engraftment
Vehicles
C/E
Add on EPZ
EPZ
EPZ + C/E
E
F
Tumor volume (mm3)
Sham - chemonaive
RT - chemonaive
Sham - chemoresistant
RT - chemoresistant
Percent survival
n.s.
Days post-treatment
G
Vehicle - chemonaive
IRI - chemonaive
Vehicle - chemoresistant
IRI - chemoresistant
p<0.0001****
H
EPZ
IRI
EPZ/IRI
I
EZP/IRI
J
Vehicle
IRI • 6 cycles
EPZ/IRI • 6 cycles
Days post-randomization
Days post-engraftment
K
Vehicle
EPZ/IRI rechallenge
L
H&E
ChrA
Synp
Ki67
Trichrome
Naive
Resistant
Vehicle
EPZ
EPZ/IRI
post-CR

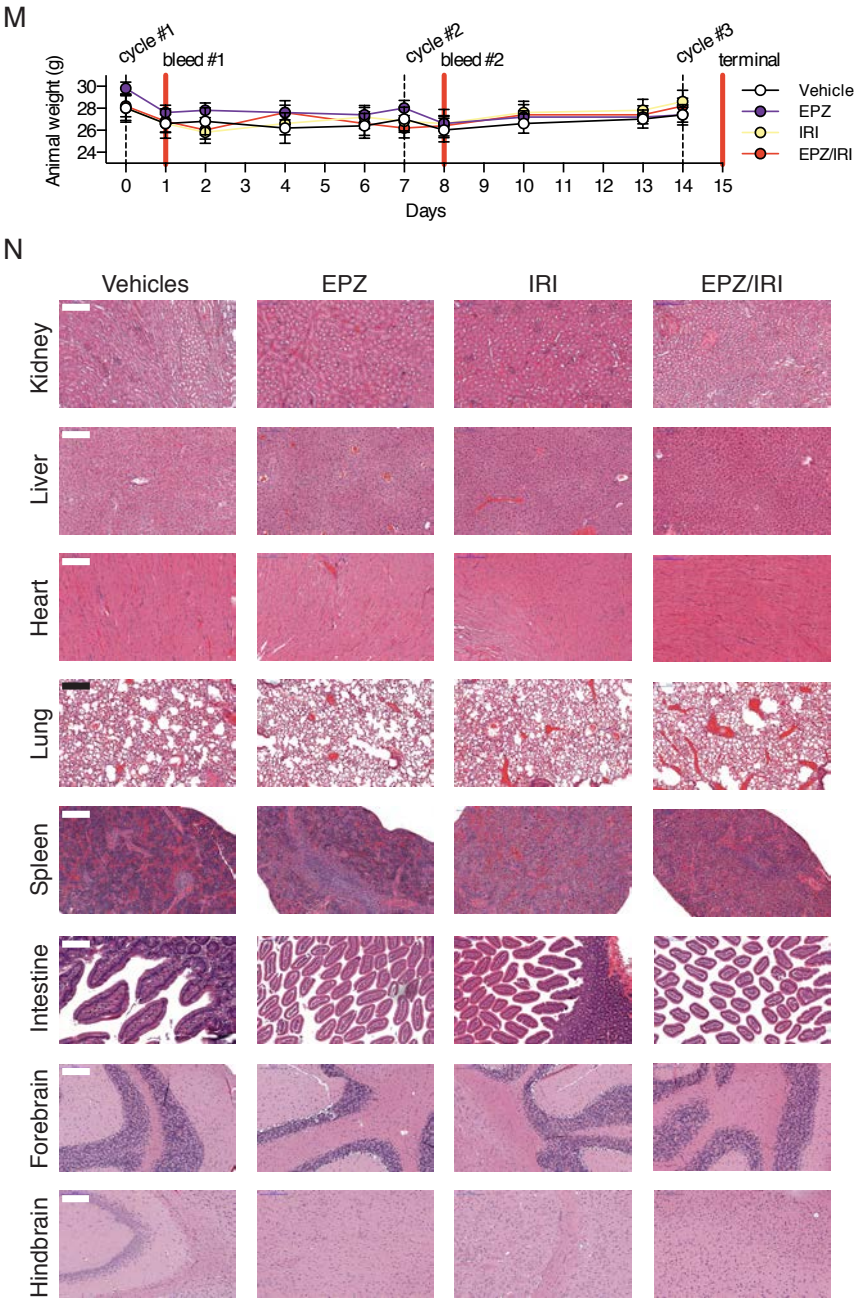

Figure S7 (related to Figure 7). Combining EPZ with chemotherapy is an effective and safe therapeutic strategy in SCLC.
(A) Quantitation of EZH2 and H3K27me3 in SCLC cell lines NCI-H446 and NCI-H69 following DNA damage. EZH2 signal normalized to actin and H3K27me3 normalized to total H3. Cells exposed to 1 μM topotecan for 1 hr and then washed and released into fresh media. Cells were collected at indicated time points for Western blot. Relative fluorescence units (RFU) per targets interrogated as shown.
(B) Quantitation of EZH2 and H3K27me3 following dose-dependent DNA damage in NCI-H446. Damage induced as in (A) using indicated doses of topotecan and then collected at time points for Western blot. Data normalized to undamaged control at 48 hr. EZH2 and H3K27me3 relative fluorescence units (RFU) shown per time point.
(C) Effect of type of DNA damaging agent on EZH2 and H3K27me3 in NCI-H446. Damage induced as in (A) using indicated doses of compounds. EZH2 and H3K27me3 relative fluorescence units (RFU) shown per time point
(D) Average animal weights on study for Figure 7D ± SEM for each treatment arm indicated. n=5/arm.
(E) Average animal weights on study for Figure 7E ± SEM for each treatment arm indicated. n=5/arm.
(F) Efficacy of ionizing radiation upon acquired resistance to C/E. Chemonaive and chemoresistant versions of SCRX-Lu149 received 2 Gy (abbreviated RT) or sham irradiation for 4 consecutive days and tumor volumes were recorded during outgrowth; Mean volume ± SEM; n=5-6/arm. Survival reported as time post-treatment to reach a volumetric endpoint of 1,000 mm^3. n.s.=non-significant by log-rank (Mantle-Cox) test.

(G) Efficacy of irinotecan upon acquired resistance to C/E. Chemonaive and chemoresistant versions of SCRX-Lu149 received weekly cycles of irinotecan (100 mg/kg IP every 7 days) or vehicle for 6 consecutive weeks and tumor volumes were recorded. Dashed horizontal lines indicate day 1 of a weekly cycle. Mean volume ± SEM; n=5/arm. P value shown for paired t-test.
(H) Average animal weights on study for Figure 7F ± SEM for each treatment arm indicated; n=5/arm.
(I) Average animal weights on study for Figure 7G ± SEM for each treatment arm indicated; n=5/arm.
(J) Efficacy of combined irinotecan (IRI) and EPZ (EPZ/IRI) in the $SLFN11^{LOW}$ chemonaive model JHU-LX108. Survival curve shown above; event/endpoint is time to tumor volume reaching 1,000 mm^3 post-randomization (on treatment). Randomizing starting volume (green dotted line) and endpoint volume (red dotted line) are indicated horizontally on tumor growth curves. Dashed lines represent day 1 of a weekly cycle, with grey area indicating time on treatment; Mean volume ± SEM; n=5/arm.
(K) Efficacy of combined irinotecan (IRI) and EPZ (EPZ/IRI) in the $SLFN11^{HIGH}$ chemonaive model JHU-LX102 as in Figure S7J. Inset*:* 4/5 animals were re-treated with 3 cycles of EPZ/IRI after recurring from complete responses (individual orange lines), treating the median volume recurrence animals with vehicle only (black line) and monitoring outgrowth.
(L) Immunohistochemistry on paired chemonaive and chemoresistant JHU-LX102 samples treated with EPZ alone or in combination with IRI. ChrA=chromogranin A, Synp=synaptophysin, Trichrome=Masson's trichrome. Scale bar on H&E panel set to 100 μm and equivalent throughout panels. All vehicle, EPZ or EPZ/IRI tumors were treated continuously for 21 days. The post-complete response (CR) tumor was the vehicle-treated median outgrowth tumor from Figure S7K inset. Three tumors were analyzed per arm by a pathologist blinded to treatment group, with the exception of the post-CR tumor (n=1). Shown are representative images from one animal per group.
(M) Schematic outline of EPZ ± IRI toxicity studies performed in 10-12 week old female NSG mice. Animal weights reported as means ± SEM; treatment arms color legend on far right. Cycles of irinotecan (dashed vertical lines; 100 mg/kg IP) were given 24 hr before tail vein bleeds, where bleeds are indicated by solid, vertical red lines. Following the final cycle of irinotecan (cycle #3), all animals were taken for gross necropsy and histologic analysis; n=5/arm.
(N) Representative H&E images of major organs examined for treatment-related toxicities. Scale bars (200 μm) are indicated on vehicle arm images and equivalent throughout panels; n=5/arm.

Table S3 (related to Figure 7). Blood chemistry for toxicity analysis of EPZ ± IRI in non-tumor bearing NSG female mice.
Provided as an excel file.

SUPPLEMENTAL EXPERIMENTAL PROCEDURES

In vitro and in vivo generation of acquired resistance to cisplatin/etoposide

Mouse DKO and TKO cells were cultured under increasing concentrations of etoposide, refreshing media and drug twice weekly, until stable cultures were capable of proliferating in the presence of 1 μM etoposide. Parental and resistant versions of the DKO and TKO cell lines were confirmed by STR, as lines were in continuous culture for ~6 months. In vivo, cohorts of tumor-bearing animals were challenged weekly with cycles of cisplatin (5 mg/kg IP day 1) and etoposide (8 mg/kg IP days 1-3) as long as the following conditions were met: 1) tumor volumes were greater than 100 mm^3 and 2) animals did not lose >20% body weight when compared to the body weights at the point of randomization (starting weights). On the morning of day 1 of each weekly cycle, animals were given 0.8-1.0 ml of normal saline subcutaneously to facilitate renal clearance of the cisplatin, as cumulative dehydration from cisplatin was the dose-limiting toxicity of this schedule. Where toxicity (usually uniform within a treatment cohort) was encountered, animals were given one week of holiday from treatment to allow recovery of weight. All NSG animals were maintained on Sulfatrim® diet throughout the period of study.

mSCLC triple knock-out allograft (TKO-A)

All in vivo mSCLC experiments were performed using an allograft of the triple (*Rb1/Trp53/Rbl2*) knockout mouse model of SCLC (Jahchan et al., 2013) maintained in female, 2-3 month old athymic nude mice (Envigo; Hsd:Athymic Nude-Foxn1nu). Flank tumors were engrafted and maintained as described for PDX models, with the exception of using a mouse tumor dissociation kit to process these tumors into single cell suspensions (Miltenyi; 130-096-730).

Tumor Micro Array (TMA) construction and immunohistochemistry

Tumor cores were obtained from embedded PDX tumors tissue in donor blocks using a 1 mm biopsy punch needle (IHC World; W-125-0) then embedded/inserted into paraffin recipient block/negative mold (IHC World; 10*17 Quick Ray mold IW-UM01-1). Empty slots were filled with blank paraffin cores. All cores were gently tamped down using biopsy punch needle then the entire block was placed face down on a glass slides and heated to 50 C for 2 hr to merge donor cores with the recipient block. Block and glass slide were then placed on ice for 30 min before sectioning. Two tissue microarrays (TMAs) made of primary and metastatic SCLC specimens were prepared from formalin-fixed paraffin-embedded (FFPE) tissue blocks following previously reported methods (Kononen et al., 1998; Ocak et al., 2010). Pathology blocks were retrieved from the archives of the Department of Pathology at Vanderbilt University Medical Center, Nashville VA Medical Center and St-Thomas Hospital in Nashville, Tennessee. They were obtained between 1996 and 2008 from patients who had surgery or bronchoscopy prior to medical treatment. SCLC diagnosis was confirmed on hematoxylin and eosin-stained (H&E) sections by an experienced lung cancer pathologist. Treatment was administered on an individualized basis according to disease stage and patient performance status (PS) as per standard of care therapy (chemotherapy and radiotherapy). All patients were followed through chart review until death or until data analysis of this manuscript. Clinical data were obtained from tumor registry and hospital charts. Studies to collect tissues were approved with patient consent and by the Institutional Review Boards at each medical center involved. Staining and H-score calculations, a weighed score that ranges from 0 - 300 and integrates IHC staining intensity and area, was performed as previously described (Lok et al., 2016).

Cell culture, in vitro viability assays and chemical inhibitors

All cell lines were obtained from the American Type Culture Collection (ATCC), were confirmed by STR (DDC Medical) and tested negative for mycoplasma (Lonza MycoAlert PLUS; LT07-710) within 6 months of use. All cell lines were maintained in RPMI-1640 supplemented with 10% FBS, 2 mM L-glutamine and 1x penicillin/streptomycin. Ex vivo cell culture of PDX tumors was performed as previously described (Poirier et al., 2015). EPZ011989 (abbreviated EPZ within text) was provided by Epizyme and formulated as previously described (Campbell et al., 2015). Cisplatin (APP), etoposide (Teva) and irinotecan (Hospira) for in vivo use were obtained from the MSKCC hospital pharmacy and formulated in normal saline immediately before use. Topotecan (Selleck Chem), GSK126 (Selleck Chem) and 5-azacitidine (Sigma) were purchased commercially and formulated in DMSO. Cell viability experiments were performed at 72 hr post-dosing, unless indicated otherwise within the text, where 1-5x10^4 viable cells were seeded in 100 μL/well of fresh media in black 96-well plates and drugs added to a final volume of 200 μL/well one day after seeding plates (Corning; 3916). Cell viability experiments were monitored using AlamarBlue (Life Technologies), allowing the reagent to develop overnight (~16 hr) before reading plates on a compatible plate reader (BioTek; Synergy Neo). Throughout the text DMSO is used as the vehicle control for in vitro or ex vivo experiments.

Plasmids and generation of lentiviral supernatants

SLFN11 (HsCD00082389) and human TWIST1 (HsCD00042456) cDNAs in pDONR vectors were purchased from DNASU plasmid repository. Mouse Twist1 cDNA was purchased from Origene (MR227370). Polymerase chain reactions (PCRs) were performed using a GeneAmp PCR System 9700 Thermocycler (Applied Biosystems). Competent Stbl3 cells were purchased from Invitrogen. Plasmids were isolated and purified from bacteria using QIAquick Spin Miniprep Kit (Qiagen). SLFN11 was cloned into plasmid pDONR221 (Life Technologies). Using primers with the following sequences 5'-TGATGATAATGATACCCAGCTTTCTTGTACAAAGTGGGCATT-3' and 5'-TCATTATCATCAATGGCCACCCCACGGAAAAATATACAGGTG-3', the pDONR201-SLFN11 plasmid was used as a PCR template to add 4 tandem stop codons between the C-terminal end of SLFN11 cDNA and the Myc-DDK tag sequence to ensure

termination after the SLFN11 cDNA translation. Site-directed mutagenesis of mouse Twist1 cDNA to the DNA-binding mutant K145E (Maia et al., 2012) was performed using a QuikChange Site-Directed Mutagenesis Kit (Agilent) and the following primers: forward 5'-GGACAAGCTGAGCGAGATTCAGACCC-3' and reverse 5'-GGGTCTGAATCTCGCTCAGCTTGTCC-3'. Gateway® cloning was performed according to manufacturer's recommendations (BP/LR clonase enzyme mixes; Life Technologies). The plasmid pLIX_402 was a gift from David Root (Addgene plasmid #41394) and pLT3GEPIR (Fellmann et al., 2013) was obtained from the MSKCC RNAi core facility. A list of tested shRNA sequences is available in Table S3. Lentiviral supernatants were generated and titered in 293T/17 cells as previously described (Lok et al., 2016; Moffat et al., 2006). Briefly, a multiplicity of infection (MOI) of ~1 was used to infect target cells in the presence of 8 μg/mL hexadimethrine bromide (polybrene). For suspension cells, viral transductions were performed in a swinging bucket rotor at 37 C for 30 min at 800 x g, before placing cells back into culture. One day later, media was changed on target cells. One day following media change, selection with puromcyin proceeded daily for 5-7 d to establish stably transduced cell cultures. Cells transduced with doxycycline-sensitive elements were maintained in tetracycline-free media (Clontech) prior to induction. Sanger sequencing of plasmids was performed by Genewiz, Inc. Nucleotide and protein sequence alignments were performed in Geneious Pro 4.7.6.

shRNA sequences

Target	Species	Text ID	97mer sequence (5'-3')
TWIST1	Human	shTWIST1.1	TGCTGTTGACAGTGAGCGCGCCCTCGGACAAGCTGAGCAATAGTGAAGC CACAGATGTATTGCTCAGCTTGTCCGAGGGCATGCCTACTGCCTCGGA
TWIST1	Human	shTWIST1.2	TGCTGTTGACAGTGAGCGACCAGGGCAAGCGCGGCAAGAATAGTGAA GCCACAGATGTATTCTTGCCGCGCTTGCCCTGGGTGCCTACTGCCTCGG A
Renilla luciferase	Sea Pansy	shRenilla	TGCTGTTGACAGTGAGCGCAGGAATTATAATGCTTATCTATAGTGAAG CCACAGATGTATAGATAAGCATTATAATTCCTATGCCTACTGCCTCGGA
Twist1	Mouse	shTwist1.1	TGCTGTTGACAGTGAGCGCGCCCTCGGACAAGCTGAGCAATAGTGAAG CCACAGATGTATTGCTCAGCTTGTCCGAGGGCATGCCTACTGCCTCGGA
Twist1	Mouse	shTwist1.2	TGCTGTTGACAGTGAGCGAACAAGCTGAGCAAGATTCAGATAGTGAAG CCACAGATGTATCTGAATCTTGCTCAGCTTGTCTGCCTACTGCCTCGGA
SLFN11	Human	shSLFN11.1	TGCTGTTGACAGTGAGCGCCAGTTGTCTGAAGATTTTGAATAGTGAAG CCACAGATGTATTCAAAATCTTCAGACAACTGTTGCCTACTGCCTCGGA
SLFN11	Human	shSLFN11.2	TGCTGTTGACAGTGAGCGATCAGTTCTTCATTATACCGTATAGTGAAGC CACAGATGTATACGGTATAATGAAGAACTGAGTGCCTACTGCCTCGGA
EZH2	Human	shEZH2.1	TGCTGTTGACAGTGAGCGAAAGAGGGAAAGTGTATGATAATAGTGAAG CCACAGATGTATTATCATACACTTTCCCTCTTCTGCCTACTGCCTCGGA
EZH2	Human	shEZH2.2	TGCTGTTGACAGTGAGCGCCGGAAATTTCCTTCTGATAAATAGTGAAG CCACAGATGTATTTATCAGAAGGAAATTTCCGATGCCTACTGCCTCGGA

In vivo irradiation

Once tumor volumes reached approximately 150 mm^3, mice were randomized to control and treatment arms. Flank irradiation was administered at 2 Gy/fraction to anesthetized mice for 4 consecutive days delivered by an X-Ray irradiator (XRAD 320, Precision X-Ray) with secondary collimation by custom lead cut-outs.

DNA/RNA extraction and sequencing

DNA and RNA were extracted from flash frozen tissue using AllPrep DNA/RNA mini kits (Qiagen; 80204), homogenizing tissue using a gentleMACS M tube containing ~2 mL of RLT Plus buffer (Qiagen; 1053393) supplemented with 2-mercaptoethanol (Fisher) and processing samples on a pre-specified RNA extraction cycle. Samples were passed through QIAshredder columns (Qiagen; 79656) and DNA and RNA components were eluted in water before storing DNA at -20 C and RNA at -80 C for future analyses. RNA library preparation (w/ polyA selection), multiplexing and sequencing on an Illumina HiSeq2500 in RapidRun mode (50 bp single end reads) was performed by Genewiz. SureSelect Human All Exon V4 and SureSelect Mouse All Exon enrichment kits (Agilent) were used for whole exome library preparation. MSK-IMPACT (Cheng et al., 2015; Wagle et al., 2012) and whole exome sequencing on most samples was performed by the MSKCC integrated genomics operation (iGO) core facility. Additional whole exome sequencing was performed at Genewiz.

Protein extraction, near-infrared Western blotting and protein quantitation

Whole cell lysates were prepared from frozen cell pellets or flash frozen tissue using radioimmunoprecipitation assay (RIPA) buffer lysis and extraction buffer (Thermo; 89901) supplemented with Halt™ protease and phosphatase inhibitor cocktail (Thermo; 78440). For extraction from frozen tissue, 50-100 mg of tissue was placed into gentleMACS M tube (Miltenyi; 130-094-392) in ~2 ml of ice-cold extraction buffer and processed using a pre-specified protein extraction cycle, followed by a 10 s sonication setup using 200V microtip sonicator set to 40% amplitude (QSonica; CL18). Crude lysates were clarified at 14,000 rpm for 10 min in a refrigerated bench top centrifuge (Eppendorf; 5340 R). Protein lysates were quantified using a micro BCA protein assay kit (Pierce; 23235) and then diluted with extraction buffer, NuPAGE® LDS sample buffer and reducing reagent (Life Technologies) prior to resolving on 4-12% Bis-Tris gradient gels. Gels were wet-transferred to 0.45 μm Immobilon-FL PVDF membrane (Millipore; IPFL00010, lot#R5GA0255H for all blots reported). All primary antibodies were incubated overnight with membranes in TBS Odyssey blocking buffer supplemented with 0.1% Tween-20 (LI-COR; 927-50000), while secondary antibodies were incubated at room temperature with agitation for 1 hr in primary blocking buffer supplemented with 0.01% SDS. Membranes were dried at 37 C and protected from light before imaging (LI-COR; Odyssey Sa). The same instrument gain settings were used for all targets examined (3.0 for 700 nm channel; 6.0 for 800 nm channel), with normalization of the 800 nm channel against the 700 nm channel, where indicated in the text or figure legend. Images were analyzed in ImageStudio (LI-COR; version 3.1.4) Recombinant GST-SLFN11 (Abnova; H00091607-P01) was used to determine the limit of detection for SLFN11 in cell lines and PDX tissue. 5 μg of total, clarified cell lysate was determined to be optimal for detection of 4 logs of dynamic range of for SLFN11 from in vivo sources.

Antibodies

Target	Source	Product#	Application	Fold Dilution
EZH2	Cell Signaling	5246	WB	1000
EZH2	Active Motif	39901	ChIP	5ug/reaction
H3K27me1	Active Motif	61015	WB	1000
H3K27me2	Cell Signaling	9728	WB	2500
H3K27me3	Active Motif	39155	WB	2500
H3K27me3	Millipore	07-449	ChIP	4ug/reaction
H3K36me3	Cell Signaling	4909	WB	1000
H3K4me3	Cell Signaling	9751	WB	1000
H3K27Ac	Active Motif	39685	WB	1000
H3K27Ac	Active Motif	39133	ChIP	4ug/reaction
actin (mouse)	Cell Signaling	3700	WB	5000
actin (rabbit)	Cell Signaling	8457	WB	5000
H3 (mouse)	Cell Signaling	14269	WB	5000
H3 (rabbit)	Cell Signaling	4499	WB	5000
vinculin	Cell Signaling	13901	WB	1000
TWIST1	Abcam	ab50887	WB	1000
SLFN11	Santa Cruz	sc-374339	WB	250
cleaved-PARP	Cell Signaling	5625	WB	1000
γH2A.X (phospho-S139)	Cell Signaling	9718	WB	1000
H2A.X	Cell Signaling	2595	WB	1000
GFP	Cell Signaling	2956	WB	5000
donkey anti-rabbit IRDye 800CW	LI-COR	926-32213	WB	25000
donkey anti-mouse IRDye 680LT	LI-COR	926-68022	WB	25000
donkey anti-mouse IRDye 800CW	LI-COR	926-32212	WB	25000
donkey anti-rabbit IRDye 680LT	LI-COR	926-68023	WB	25000
SLFN11	Santa Cruz	sc-374339	IHC	2ug/mL
Chromogranin A	Ventana	LK2H10	IHC	2000
Synaptophysin	BIOGENEX	Snp88	IHC	2000
Ki67/MIB1	DAKO	M7240	IHC	200

Mutation and copy number analysis

Raw reads were aligned to a custom hybrid reference genome using BWA 0.7.12-r1039 with default settings (Li and Durbin, 2009). The hybrid index was generated using a FASTA file consisting of all human GRCh38 and mouse GRCm38.p3 reference contigs as previously described (Schneeberger et al., 2016). Mapped reads were piped to SAMBLASTER 0.1.22 and samtools 1.2 for on-the-fly duplicate removal and sorting, respectively. Sorted reads were processed through the Genome Analysis Toolkit (GATK) 3.6, according to standard practices, including generation of depth of coverage analysis statistics (DePristo et al., 2011; McKenna et al., 2010). Each sample was genotyped at >1,000 common SNP sites using HaplotypeCaller to generate a fingerprint. SNP concordance was confirmed by bcftools 1.2. Mutations and indels were called using MuTect2 and annotated with the subset of common SNPs in dbSNP 147 found in >1% of the population. Variants that did not pass a MuTect2 filter, had a variant frequency <10%, or were a common SNP were excluded. Filtered mutations were annotated with snpEff (Cingolani et al., 2012). Final mutations and their annotations were loaded into the R statistical computing environment for final analysis. For novel mutation discovery, genes were

rank ordered by the number of models in which a gene was mutated in the chemoresistant setting, but not the chemonaive setting. Mutational signature data was generated by deconstructSigs v1.8.0 (Rosenthal et al., 2016). Copy number data was generated using FACETS v0.3.30 (Shen and Seshan, 2016). Copy number plots were generated using the copynumber package for R (Nilsen et al., 2012).

Gene expression analysis

Raw reads were aligned to a custom hybrid reference genome using STAR 2.4.1b (Dobin et al., 2013). The hybrid index was generated using a FASTA file consisting of all human GRCh38 and mouse GRCm38.p3 reference contigs and the human GENCODE gene set release 20 transcript model as previously described (Schneeberger et al., 2016). Mapped reads were assigned to GENCODE 20 genes using Subread 1.5.0-p2 to generate a raw counts table (Liao et al., 2014). Raw counts were read into the R statistical computing environment for further analysis (R Core Team (2016). R: A language and environment for statistical computing. R Foundation for Statistical Computing, Vienna, Austria. URL: https://www.R-project.org/). Downstream analysis was performed with the limma package for R (Ritchie et al., 2015). Genes with ≥5 counts per million in ≥3 samples were considered for analysis. Counts were normalized to library size and transformed to log2 counts per million with upper quartile normalization. Weights were calculated based on a combination of observational-level weights determined from an estimate of the mean-variance relationship within all samples and sample-level weights reflecting the degree to which each sample follows the linear model (Ritchie et al., 2006). A linear model was fit for each contrast and standard errors were moderated using an empirical Bayes method. T statistics, B statistics, and p values were generated for each gene. P values were corrected for multiple testing by the method of Bonferroni. To identify genes with biologically significant effect sizes, statistically significant p values, and recurrent alterations, we chose to highlight genes with a fold change of ≥1.5 that were significant in ≥3 models.

Robust Multi-array Average (RMA) and quantile normalized gene expression microarray data for 1,037 cancer cell lines was downloaded from the Cancer Cell Line Encyclopedia (Barretina et al., 2012). The gene expression signal distribution of *SLFN11* is distinctly bimodal. The minor mode comprises cell lines in which the gene is not expressed while the major mode, having a greater standard deviation, comprises cell lines in which *SLFN11* is expressed at varying levels. To discriminate between cell lines based on *SLFN11* expression, a gene expression cutoff was established using two independent approaches: the method of Zilliox et al. (Zilliox and Irizarry, 2007), which estimates a gene expression cutoff based on the standard deviation of the minor mode based on the left side of the mean, and by fitting a finite mixture of 2 Gaussian components. Both approaches were in agreement in establishing a cutoff of 5.

ChIP-seq and ChIP-qPCR

Tumor tissue was submersed 1% formaldehyde in PBS, cut into small pieces and incubated at room temperature for 15 min. Fixation was stopped by the addition of 0.125 M glycine (final concentration). The tissue pieces were then treated with a TissueTearer and finally spun down and washed twice in PBS. Chromatin was isolated by the addition of lysis buffer, followed by disruption with a Dounce homogenizer. NCI-H446 cells were fixed with 1% formaldehyde for 15 min and quenched with 0.125 M glycine. Chromatin was isolated by the addition of lysis buffer, followed by disruption with a Dounce homogenizer. Lysates were sonicated and the DNA sheared to an average length of 300-500 bp. Genomic DNA (Input) was prepared by treating aliquots of chromatin with RNase, proteinase K and heat for de-crosslinking, followed by ethanol precipitation. Pellets were re-suspended and the resulting DNA was quantified on a NanoDrop spectrophotometer. Extrapolation to the original chromatin volume allowed quantitation of the total chromatin yield. Aliquots of chromatin (20-30 µg) were pre-cleared with protein A agarose beads (Invitrogen). Genomic DNA regions of interest were isolated using 5 µl antibody against EZH2 (Active Motif; 39901), or 4 µg of antibody against H3K27Ac (Active Motif; 39133) and H3K27me3 (Millipore; 07-449). Complexes were washed, eluted from the beads with SDS buffer, and subjected to RNase and proteinase K treatment. Crosslinks were reversed by incubation overnight at 65 C, and ChIP DNA was purified by phenol-chloroform extraction and ethanol precipitation. Quantitative PCR (qPCR) reactions were carried out by Active Motif in triplicate using SYBR Green Supermix (Bio-Rad; 170-8882) on a CFX Connect™ Real Time PCR system. The *SLFN11* primer pair targeting upstream of the first exon are as follows: forward 5'-CGAGCCAGAGTGGGATTTAAC-3' and reverse 5'-TTTCATATCACTAGCAGCGTGAC-3'. The resulting signals were normalized for primer efficiency by carrying out qPCR for each primer pair using Input DNA (pooled unprecipitated DNA from cells or tissues). Test sites were run alongside the positive control sites targeted to the *ACTB* promoter (Active Motif; 71023) and *CCND2* gene (Active Motif; 71008) and a negative control primer pair that amplifies a region in a gene desert on chromosome 12 (Active Motif; 71001). For *SLFN11* exon-by-exon ChIP-qPCR, the following primers were used: exon 1 forward 5'-CACGGGTAGAAACGCAACTC-3' and reverse 5'-GCTGGAGCTTGAGAGGTCAG-3', exon 2 forward 5'-GAAACAAAAGCACCTGATTCTAGTC-3' and reverse 5'-TTGGTGGGAACTCTGGCTAC-3', exon 3 forward 5'-TTCTTACCACCTTGCCTAGTTTAG-3' and reverse 5'-TGGTCTTGGAATGCAGAATG-3', exon 4 forward 5'-TTGGCTTCCTTTTGGTCTTC-3' and reverse 5'-CTTTGCAGCCTCAGTTCTTC-3', exon 5 forward 5'-GCAGAGCACTTTCAGGATTTTAC-3' and reverse 5'-TCTCAACACCAGCCAGTTTC-3', exon 6 5'-CAAAATTCCCCGAAAGAAAG-3' and reverse 5'-CTCTGGAGGGACCTGATCTC-3', and exon 7 5'-TCATTTCATCTTGGCCTATAATTTC-3' and reverse 5'-TGGTCTCCAGAGCTTGTTCTC-3'. Data are reported as "binding events per 1000 cells" which considers chromatin input, ChIP volumes and primer pair efficiencies. Illumina sequencing libraries were prepared from the ChIP and Input DNAs by the standard consecutive enzymatic steps of end-polishing, dA-addition, and adaptor ligation. After a final PCR amplification step, the resulting DNA libraries were quantified and sequenced on Illumina's NextSeq 500 (75 bp single ended reads). Reads were aligned to the human

genome (hg19) using BWA (Li and Durbin, 2009) algorithm (default settings). Duplicate reads were removed and only uniquely mapped reads (mapping quality ≥25) were used for further analysis. Alignments were extended in silico at their 3'-ends to a length of 200 bp, which is the average genomic fragment length in the size-selected library, and assigned to 32 bp bins along the genome. The resulting histograms (genomic "signal maps") were stored in bigWig files. ChIP target enriched regions were identified using the SICER (Zang et al., 2009) algorithm (FDR $1E^{-10}$, gap = 600 bp). Drosophila genome spike-in was used to downsample and normalize tag counts for comparisons across treated and untreated samples (Active Motif; ChIP Normalization Strategy) (Orlando et al., 2014). For the spike-in adjusted analysis, the downscaling of H3K27me3 in the EPZ-treated samples was >5-fold, compared to the vehicle controls. In addition, the resistant vehicle H3K27Ac data was downscaled by ~2.5-fold as compared to all other samples. The EZH2 data was only normalized by <1.5-fold across all samples based on the spike-in tag counts. All plots were generated using the R statistical computing environment.

SUPPLEMENTAL REFERENCES

Campbell, J. E., Kuntz, K. W., Knutson, S. K., Warholic, N. M., Keilhack, H., Wigle, T. J., Raimondi, A., Klaus, C. R., Rioux, N., Yokoi, A.*, et al.* (2015). EPZ011989, A Potent, Orally-Available EZH2 Inhibitor with Robust in Vivo Activity. ACS Med Chem Lett *6*, 491-495.

Cheng, D. T., Mitchell, T. N., Zehir, A., Shah, R. H., Benayed, R., Syed, A., Chandramohan, R., Liu, Z. Y., Won, H. H., Scott, S. N.*, et al.* (2015). Memorial Sloan Kettering-Integrated Mutation Profiling of Actionable Cancer Targets (MSK-IMPACT): A Hybridization Capture-Based Next-Generation Sequencing Clinical Assay for Solid Tumor Molecular Oncology. J Mol Diagn *17*, 251-264.

Cingolani, P., Platts, A., Wang le, L., Coon, M., Nguyen, T., Wang, L., Land, S. J., Lu, X., and Ruden, D. M. (2012). A program for annotating and predicting the effects of single nucleotide polymorphisms, SnpEff: SNPs in the genome of Drosophila melanogaster strain w1118; iso-2; iso-3. Fly (Austin) *6*, 80-92.

DePristo, M. A., Banks, E., Poplin, R., Garimella, K. V., Maguire, J. R., Hartl, C., Philippakis, A. A., del Angel, G., Rivas, M. A., Hanna, M.*, et al.* (2011). A framework for variation discovery and genotyping using next-generation DNA sequencing data. Nat Genet *43*, 491-498.

Dobin, A., Davis, C. A., Schlesinger, F., Drenkow, J., Zaleski, C., Jha, S., Batut, P., Chaisson, M., and Gingeras, T. R. (2013). STAR: ultrafast universal RNA-seq aligner. Bioinformatics *29*, 15-21.

Fellmann, C., Hoffmann, T., Sridhar, V., Hopfgartner, B., Muhar, M., Roth, M., Lai, D. Y., Barbosa, I. A., Kwon, J. S., Guan, Y.*, et al.* (2013). An optimized microRNA backbone for effective single-copy RNAi. Cell Rep *5*, 1704-1713.

Hann, C. L., Daniel, V. C., Sugar, E. A., Dobromilskaya, I., Murphy, S. C., Cope, L., Lin, X., Hierman, J. S., Wilburn, D. L., Watkins, D. N., and Rudin, C. M. (2008). Therapeutic efficacy of ABT-737, a selective inhibitor of BCL-2, in small cell lung cancer. Cancer Res *68*, 2321-2328.

Jahchan, N. S., Dudley, J. T., Mazur, P. K., Flores, N., Yang, D., Palmerton, A., Zmoos, A. F., Vaka, D., Tran, K. Q., Zhou, M.*, et al.* (2013). A drug repositioning approach identifies tricyclic antidepressants as inhibitors of small cell lung cancer and other neuroendocrine tumors. Cancer Discov *3*, 1364-1377.

Kononen, J., Bubendorf, L., Kallioniemi, A., Barlund, M., Schraml, P., Leighton, S., Torhorst, J., Mihatsch, M. J., Sauter, G., and Kallioniemi, O. P. (1998). Tissue microarrays for high-throughput molecular profiling of tumor specimens. Nat Med *4*, 844-847.

Leong, T. L., Marini, K. D., Rossello, F. J., Jayasekara, S. N., Russell, P. A., Prodanovic, Z., Kumar, B., Ganju, V., Alamgeer, M., Irving, L. B.*, et al.* (2014). Genomic characterisation of small cell lung cancer patient-derived xenografts generated from endobronchial ultrasound-guided transbronchial needle aspiration specimens. PLoS One *9*, e106862.

Li, H., and Durbin, R. (2009). Fast and accurate short read alignment with Burrows-Wheeler transform. Bioinformatics *25*, 1754-1760.

Liao, Y., Smyth, G. K., and Shi, W. (2014). featureCounts: an efficient general purpose program for assigning sequence reads to genomic features. Bioinformatics *30*, 923-930.

Lok, B. H., Gardner, E. E., Schneeberger, V. E., Ni, A., Desmeules, P., Rekhtman, N., de Stanchina, E., Teicher, B. A., Riaz, N., Powell, S. N.*, et al.* (2016). PARP Inhibitor Activity Correlates with SLFN11 Expression and Demonstrates Synergy with Temozolomide in Small Cell Lung Cancer. Clin Cancer Res.

McKenna, A., Hanna, M., Banks, E., Sivachenko, A., Cibulskis, K., Kernytsky, A., Garimella, K., Altshuler, D., Gabriel, S., Daly, M., and DePristo, M. A. (2010). The Genome Analysis Toolkit: a MapReduce framework for analyzing next-generation DNA sequencing data. Genome Res *20*, 1297-1303.

Moffat, J., Grueneberg, D. A., Yang, X., Kim, S. Y., Kloepfer, A. M., Hinkle, G., Piqani, B., Eisenhaure, T. M., Luo, B., Grenier, J. K.*, et al.* (2006). A lentiviral RNAi library for human and mouse genes applied to an arrayed viral high-content screen. Cell *124*, 1283-1298.

Nilsen, G., Liestol, K., Van Loo, P., Moen Vollan, H. K., Eide, M. B., Rueda, O. M., Chin, S. F., Russell, R., Baumbusch, L. O., Caldas, C.*, et al.* (2012). Copynumber: Efficient algorithms for single- and multi-track copy number segmentation. BMC Genomics *13*, 591.

Ocak, S., Yamashita, H., Udyavar, A. R., Miller, A. N., Gonzalez, A. L., Zou, Y., Jiang, A., Yi, Y., Shyr, Y., Estrada, L.*, et al.* (2010). DNA copy number aberrations in small-cell lung cancer reveal activation of the focal adhesion pathway. Oncogene *29*, 6331-6342.

Orlando, D. A., Chen, M. W., Brown, V. E., Solanki, S., Choi, Y. J., Olson, E. R., Fritz, C. C., Bradner, J. E., and Guenther, M. G. (2014). Quantitative ChIP-Seq normalization reveals global modulation of the epigenome. Cell Rep *9*, 1163-1170.

Poirier, J. T., Dobromilskaya, I., Moriarty, W. F., Peacock, C. D., Hann, C. L., and Rudin, C. M. (2013). Selective tropism of Seneca Valley virus for variant subtype small cell lung cancer. J Natl Cancer Inst *105*, 1059-1065.

Ritchie, M. E., Diyagama, D., Neilson, J., van Laar, R., Dobrovic, A., Holloway, A., and Smyth, G. K. (2006). Empirical array quality weights in the analysis of microarray data. BMC Bioinformatics *7*, 261.

Ritchie, M. E., Phipson, B., Wu, D., Hu, Y., Law, C. W., Shi, W., and Smyth, G. K. (2015). limma powers differential expression analyses for RNA-sequencing and microarray studies. Nucleic Acids Res *43*, e47.

Rosenthal, R., McGranahan, N., Herrero, J., Taylor, B. S., and Swanton, C. (2016). DeconstructSigs: delineating mutational processes in single tumors distinguishes DNA repair deficiencies and patterns of carcinoma evolution. Genome Biol *17*, 31.

Saunders, L. R., Bankovich, A. J., Anderson, W. C., Aujay, M. A., Bheddah, S., Black, K., Desai, R., Escarpe, P. A., Hampl, J., Laysang, A.*, et al.* (2015). A DLL3-targeted antibody-drug conjugate eradicates high-grade pulmonary neuroendocrine tumor-initiating cells in vivo. Sci Transl Med *7*, 302ra136.

Shen, R., and Seshan, V. E. (2016). FACETS: allele-specific copy number and clonal heterogeneity analysis tool for high-throughput DNA sequencing. Nucleic Acids Res *44*, e131.

Wagle, N., Berger, M. F., Davis, M. J., Blumenstiel, B., Defelice, M., Pochanard, P., Ducar, M., Van Hummelen, P., Macconaill, L. E., Hahn, W. C.*, et al.* (2012). High-throughput detection of actionable genomic alterations in clinical tumor samples by targeted, massively parallel sequencing. Cancer Discov *2*, 82-93.

Zang, C., Schones, D. E., Zeng, C., Cui, K., Zhao, K., and Peng, W. (2009). A clustering approach for identification of enriched domains from histone modification ChIP-Seq data. Bioinformatics *25*, 1952-1958.

Zilliox, M. J., and Irizarry, R. A. (2007). A gene expression bar code for microarray data. Nat Methods *4*, 911-913.